Inorg. Chem. **2005**, *44*, 4786–4795

Proton Electroreduction Catalyzed by Cobaloximes: Functional Models for Hydrogenases

Mathieu Razavet, Vincent Artero,* and Marc Fontecave

Laboratoire de Chimie et Biochimie des Centres Rédox Biologiques, UMR 5047 CEA/CNRS/Université Joseph Fourier, CEA-Grenoble, DRDC/CB, Bat K', 17 rue des Martyrs, 38054 Grenoble Cedex 09, France

Received February 1, 2005

Cobaloximes have been examined as electrocatalysts for proton reduction in nonaqueous solvent in the presence of triethylammonium chloride. $[Co^{III}(dmgH)_2pyCl]$, working at moderate potentials (–0.90 V/(Ag/AgCl/3 mol•L^{-1} NaCl) and in neutral conditions, is a promising catalyst as compared to other first-row transition metal complexes which generally function at more negative potentials and/or at lower pH. More than 100 turnovers can be achieved during controlled-potential electrolysis without detectable degradation of the catalyst. Cyclic voltammograms simulation is consistent with a heterolytic catalytic mechanism and allowed us to extract related kinetic parameters. Introduction of an electron-donating (electron-withdrawing) substituent in the axial pyridine ligand significantly increases (decreases) the rate constant of the catalytic cycle determining step. This effect linearly correlates with the Hammet coefficients of the introduced substituents. The influence of the equatorial glyoxime ligand was also investigated and the capability of the stabilized BF_2-bridged species $[Co(dmgBF_2)_2(OH_2)_2]$ for electrocatalyzed hydrogen evolution confirmed.

Introduction

Because its combustion in fuel cells does not exhaust greenhouse gas, hydrogen is expected to become a major energetic vector in the next century.[1] However, its production is currently not sufficient to sustain the world economy and is mainly achieved through nonecological fossil fuel reforming processes. Alternatively, biomass pyrolysis and water splitting, in thermolytic, electrolytic, or photolytic pathways, can afford hydrogen as a carbon-neutral fuel, although this is not yet cost-effective. Regarding water electrolysis, whatever the power supplied, two technologies for hydrogen production are currently economically viable on a small scale: alkaline electrolyzers using nickel cathodes and PEM devices using unsustainable noble metals such as platinum as the electrocatalyst. The latter is the most promising for various reasons, but it suffers from the costs of both the membrane and the noble metal, which cannot be reduced at the moment.[2] The development of new catalysts for the hydrogen evolution reaction (*her*) based on cheap first-row transition metals has been a long-term goal for inorganic chemists.[3] This was recently boosted up by the single-crystal structure resolution of the hydrogenases enzymes which revealed the composition of their active sites.[4] Hydrogenases are indeed the only molecular catalysts capable of catalyzing both proton reduction and hydrogen oxidation with efficiencies comparable to platinum.[5] These reactions proceed at fascinating binuclear active sites based on iron only ([Fe]-only H_2ase) or both nickel and iron ([FeNi] H_2ase) metal ions coordinating cyanide (CN^-) and carbon monoxide (CO) ligands in a sulfur-rich environment (Figure 1).[4] Intense work was exquisitely and successfully done in the past few years to synthesize biomimetic models of [Fe]-only H_2ase retaining the sulfur environment, the nature, and number of metal ions as well as the diatomic carbonyl and cyanide ligands found at the active site.[6−12] The activities, displayed by some of

* Author to whom correspondence should be addressed. E-mail: vartero@cea.fr. Phone: int + 4 38 78 91 06. Fax: int + 4 38 78 91 24.

(1) Towards A Hydrogen Economy (special issue). *Science* **2004**, *305*, 13 (Aug).
(2) Turner, J. A. *Science* **2004**, *305*, 972.
(3) (a) Artero, V.; Fontecave, M. *Coord. Chem. Rev.*, published online Feb 23, 2005, 10.1016/j.ccr.2005.01.014. (b) Kölle, U. *New. J. Chem.* **1992**, *16*, 157.
(4) [Fe]-only hydrogenases: (a) Peters, J. W.; Lanzilotta, W. N.; Lemon, B. J.; Seefeldt, L. C. *Science* **1998**, *282*, 1853. (b) Nicolet, Y.; Piras, C.; Legrand, P.; Hatchikian, C. E.; Fontecilla-Camps, J. C. *Structure* **1999**, *7*, 13. [NiFe] hydrogenases: (c) Volbeda, A.; Charon, M. H.; Piras, C.; Hatchikian, E. C.; Frey, M.; Fontecilla-Camps, J. C. *Nature* **1995**, *373*, 580. (d) Volbeda, A.; Garcin, E.; Piras, C.; de Lacey, A. L.; Fernandez, V. M.; Hatchikian, E. C.; Frey, M.; Fontecilla-Camps, J. C. *J. Am. Chem. Soc.* **1996**, *118*, 12989. (e) Higuchi, Y.; Yagi, T.; Yasuoka, N. *Structure* **1997**, *5*, 1671. (f) Higuchi, Y.; Ogata, H.; Miki, K.; Yasuoka, N.; Yagi, T. *Structure* **1999**, *7*, 549.
(5) Jones, A. K.; Sillery, E.; Albracht, S. P. J.; Armstrong, F. A. *Chem. Commun*. **2002**, 866.

10.1021/ic050167z CCC: $30.25
Published on Web 06/02/2005

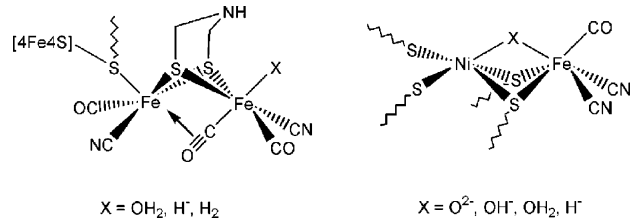

X = OH_2, H^-, H_2 X = O^{2-}, OH^-, OH_2, H^-

Figure 1. Structures of the active sites of [Fe]-only (left) and [NiFe] (right) hydrogenases. (X are putative ligands.)

these compounds,[6c,d,7c,g,i−k,8h,i,9] are noteworthy but still lie below those obtained with former nonbiomimetic catalysts such as $[Cp^*Rh(bipy)(OH_2)]^{2+}$,[13] $[Ni(biscyclam)]^{4+}$,[14] cobaloximes,[15] cobalt porphyrins,[16] and related complexes.[17]

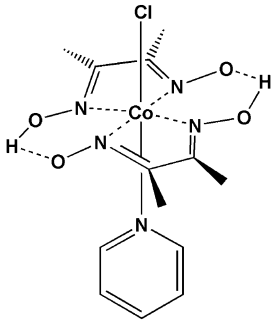

Figure 2. $[Co(dmgH)_2(py)Cl]$.

Moreover, biomimics of [Fe]-only H_2ase sometimes suffer from their instability[8h] since they generally lack chelating ligands which contribute to the stability of the coordination sphere during catalysis.[3] On the other hand, the fine combination of soft ligands found at the active site probably helps making the iron center nucleophilic and easily reducible, stabilizing an open coordination site for substrate binding. Some of these features can be found in cobaloximes, which have proved to be interesting electrocatalysts for *her* in terms of both cost and working potential.

Cobaloximes (Figure 2) are pseudomacrocyclic bis(dialkylglyoximato)cobalt complexes. They were first developed to mimic vitamin B_{12} and related compounds.[18] In the reduced Co(I) state, they are known as powerful nucleophiles. They can be protonated to yield cobalt(III)−hydride species, which can further evolve dihydrogen through either protonation of the hydride moiety or bimolecular reductive elimination.[19] However, their catalytic activity for *her* was only described twice, first using divalent metal salts as bulk reducing agents in strongly acidic media[15a] and second in nonaqueous solvent in combination with $[Ru(bipy)_3]^{2+}$ as a photosensitizer.[15b] We report here a systematic study of proton electroreduction catalyzed by cobaloximes at glassy carbon electrodes.

Experimental Section

Materials. Commercial EPR-grade DMF and electronic-grade 1,2-dichloroethane were degassed by bubbling nitrogen. Tetrahydrofuran was distilled from sodium−benzophenone and kept under argon. Cobalt chloride hexahydrate (Acros), cobalt acetate tetrahydrate (Strem chemicals), glyoxime (gH_2) (Lancaster), dimethylglyoxime ($dmgH_2$) (Acros), diphenylglyoxime ($dpgH_2$) (Aldrich), 4-(dimethylamino)pyridine (Aldrich), triethylammonium chloride (Acros), triethylamine (Acros), and tetrafluoroboric acid diethyl ether complex (Fluka) were used as received. The supporting electrolyte (n-$Bu_4N)BF_4$ was prepared from (n-$Bu_4N)HSO_4$ (Aldrich) and $NaBF_4$ (Aldrich) and dried overnight at 80 °C under vacuum.

$[Co(dmgH)_2(py)Cl]$,[20] $[Co(dmgH)_2(OH_2)_2]$,[20] $[Co(dmgH)_2(py)_2](PF_6)$,[21] $[Co(dmgBF_2)_2(OH_2)_2]$,[22] $[Co(gH)_2(py)Cl]$,[23] $[Co(dmgH)_2(PBu_3)Cl]$,[23] $[Co(dpgH)_2(py)Cl]$,[20] isonicotinoyl chloride hydrochloride,[24] and $(Et_3NH)BF_4$[25] were prepared as previously described.

(6) (a) Schmidt, M.; Contakes, S. M.; Rauchfuss, T. B. *J. Am. Chem. Soc.* **1999**, *121*, 9736. (b) Gloaguen, F.; Lawrence, J. D.; Schmidt, M.; Wilson, S. R.; Rauchfuss, T. B. *J. Am. Chem. Soc.* **2001**, *123*, 12518. (c) Gloaguen, F.; Lawrence, J. D.; Rauchfuss, T. B. *J. Am. Chem. Soc.* **2001**, *123*, 9476. (d) Gloaguen, F.; Lawrence, J. D.; Rauchfuss, T. B.; Bénard, M.; Rohmer, M.-M. *Inorg. Chem.* **2002**, *41*, 6573. (e) Lawrence, J. D.; Li, H.; Rauchfuss, T. B.; Bénard, M.; Rohmer, M.-M. *Angew. Chem., Int. Ed.* **2001**, *40*, 1768. (f) Lawrence, J. D.; Li, H.; Rauchfuss, T. B. *Chem. Commun.* **2001**, 1482. (g) Li, H.; Rauchfuss, T. B. *J. Am. Chem. Soc.* **2002**, *124*, 726. (h) Lawrence, J. D.; Rauchfuss, T. B.; Wilson, S. R. *Inorg. Chem.* **2002**, *41*, 6193. (i) Boyle, C. A.; Rauchfuss, T. B.; Wilson, S. R.; Rohmer, M.-M.; Bénard, M. *J. Am. Chem. Soc.* **2004**, *126*, 15151. (j) Rauchfuss, T. B. *Inorg. Chem*. **2004**, *43*, 14.

(7) (a) Lyon, E. J.; Georgakaki, I. P.; Reibenspies, J. H.; Darensbourg, M. Y. *Angew. Chem., Int. Ed.* **1999**, *38*, 3178. (b) Lyon, E. J.; Georgakaki, I. P.; Reibenspies, J. H.; Darensbourg, M. Y. *J. Am. Chem. Soc.* **2001**, *123*, 3268. (c) Zhao, X.; Georgakaki, I. P.; Miller, M. L.; Yarbrough, J. C.; Darensbourg, M. Y. *J. Am. Chem. Soc.* **2001**, *123*, 9710. (d) Darensbourg, M. Y.; Lyon, E. J.; Zhao, X.; Georgakaki, I. P. *Proc. Natl. Acad. Sci. U.S.A.* **2003**, *100*, 3683. (e) Georgakaki, I. P.; Thomson, L. M.; Lyon, E. J.; Hall, M. B.; Darensbourg, M. Y. *Coord. Chem. Rev.* **2003**, *238*−*239*, 255. (f) Zhao, X.; Georgakaki, I. P.; Miller, M. L.; Yarbrough, J. C.; Darensbourg, M. Y. *J. Am. Chem. Soc.* **2001**, *123*, 9710. (g) Zhao, X.; Georgakaki, I. P.; Miller, M. L.; Mejia-Rodriguez, R.; Chiang, C.-Y.; Darensbourg, M. Y. *Inorg. Chem.* **2002**, *41*, 3917. (h) Zhao, X.; Chiang, C.-Y.; Miller, M. L.; Rampersad, M. V.; Darensbourg, M. Y. *J. Am. Chem. Soc.* **2004**, *125*, 518. (i) Georgakaki, I. P.; Miller, M. L.; Darensbourg, M. Y. *Inorg. Chem.* **2003**, *42*, 2489. (j) Chong, D.; Georgakaki, I. P.; Mejia-Rodriguez, R.; Sanabria-Chinchilla, J.; Soriaga, M. P.; Darensbourg, M. Y. *Dalton Trans.* **2003**, 4158. (k) Meija-Rodriguez, R.; Chong, D.; Reibenspies, J. H.; Soriaga, M. P.; Darensbourg, M. Y. *J. Am. Chem. Soc.* **2004**, *126*, 12004.

(8) (a) Le Cloirec, A.; Best, S. P.; Borg, S.; Davies, S. C.; Evans, D. J.; Hughes, D. L.; Pickett, C. J. *Chem. Commun.* **1999**, 2285. (b) Razavet, M.; Le Cloirec, A.; Davies, S. C.; Hughes, D. L.; Pickett, C. J. *J. Chem. Soc., Dalton Trans.* **2001**, 3551. (c) Razavet, M.; Davies, S. C.; Hughes, D. L.; Pickett, C. J. *Chem. Commun.* **2001**, 847. (d) Razavet, M.; Borg, S. J.; Georges, S. J.; Best, S. P.; Fairhurst, S. A.; Pickett, C. J. *Chem. Commun.* **2002**, 700. (e) Georges, S. J.; Cui, Z.; Razavet, M.; Pickett, C. J. *Chem.*−Eur. J. **2002**, *8*, 4037. (f) Yang, X.; Razavet, M.; Wang, X.-B.; Pickett, C. J.; Wang, L.-S. *J. Phys. Chem.* A **2003**, *107*, 4612. (g) Evans, D. J.; Pickett, C. J. *Chem. Soc. Rev.* **2003**, *32*, 268. (h) Borg, S. J.; Behrsing, T.; Best, S. P.; Razavet, M.; Liu, X.; Pickett, C. J. *J. Am. Chem. Soc.* **2004**, *126*, 16988. (i) Tard, C.; Liu, X.; Hughes, D. L.; Pickett, C. J. *Chem. Commun.* **2005**, 133. (j) Zampella, G.; Bruschi, M.; Fantucci, P.; Razavet, M.; Pickett, C. J.; De Gioia, L. *Chem.*−Eur. J. **2005**, *11*, 509.

(9) Ott, S.; Kritikos, M.; Ackermark, B.; Sun, L.; Lomoth, R. *Angew. Chem., Int. Ed.* **2004**, *43*, 1006.

(10) Nehring, J. L.; Heinekey, D. M. *Inorg. Chem.* **2003**, *42*, 4288.

(11) Das, P.; Capon, J.-F.; Gloagen, F.; Pétillon, F. Y.; Schollhammer, P.; Talarmin, J. *Inorg. Chem.* **2004**, *43*, 8203.

(12) Song, L.-C.; Yang, Z.-Y.; Bian, H.-Z.; Hu, Q.-M. *Organometallics* **2004**, *23*, 3082.

(13) (a) Kölle, U.; Grätzel, M. *Angew. Chem., Int. Ed. Engl.* **1987**, *26*, 567. (b) Kölle, U.; Kang, B.-S.; Infelta, P.; Comte, P.; Grätzel, M. *Chem. Ber.* **1989**, *122*, 1869. (c) Cosnier, S.; Deronzier, A.; Vlachopoulos, N. *J. Chem. Soc., Chem. Commun.* **1989**, 1259.

(14) Collin, J.-P.; Jouaiti, A.; Sauvage, J.-P. *Inorg. Chem.* **1988**, *27*, 1986.

(15) (a) Connolly, P.; Espenson, J. H. *Inorg. Chem.* **1986**, *25*, 2684. (b) Hawecker, J.; Lehn, J.-M.; Ziessel, R. *Nouv. J. Chim.* **1983**, *7*, 271.

(16) (a) Kellett, R. M.; Spiro, T. G. *Inorg. Chem.* **1985**, *24*, 2373. (b) Kellett, R. M.; Spiro, T. G. *Inorg. Chem.* **1985**, *24*, 2378.

(17) Fisher, B.; Eisenberg, R. *J. Am. Chem. Soc.* **1980**, *102*, 7363.

(18) Schrauzer, G. N. *Acc. Chem. Res.* **1968**, *1*, 97.

(19) Chao, T.-H.; Espenson, J. H. *J. Am. Chem. Soc.* **1978**, *100*, 129.

(20) Schrauzer, G. N. *Inorg. Synth.* **1968**, *11*, 61.

$[Co(dmgH)_2(py)I]$ was prepared as $[Co(dmgH)_2(py)Cl]$, starting from a mixture of $Co(OAc)_2 \cdot 4H_2O$ and 2 equiv of NaI instead of $CoCl_2 \cdot 2H_2O$.

Methods and Instrumentation. ^1H NMR spectra were recorded at room temperature using $CDCl_3$ or acetone-d_6 in 5 mm o.d. tubes with a 300 MHz Bruker AC300 spectrometer equipped with a QNP probehead. Electronic spectra are recorded on a diode-array HP 845x UV−visible system. Elemental analyses were performed by the Service Central d'Analyse of the CNRS (Vernaison, France). All electrochemical measurements were carried under nitrogen in a thermostated cell at 20 °C. A three-electrode cell consisting of a glassy carbon (3 mm i.d.) or platinum (2 mm i.d.) disk working electrode (Radiometer), an auxiliary platinum wire, and an Ag/AgCl/3 mol·L^{-1} NaCl reference electrode, abbreviated as (Ag/AgCl), was used. Using this reference electrode, the $(E_{pa} + E_{pc})/2$ value for the Fc/Fc^+ couple is measured in DMF (CH_3CN and 1,2-dichloroethane) at 0.55 V (0.45 and 0.47 V) on both platinum or glassy carbon electrodes. The Fc^+/Fc couple ($E° = 0.400$ V vs SHE)[26] can be used to quote potentials to SHE, when needed. Cyclic voltamograms were recorded on a EG&G PAR 273A instrument. Solution concentrations were ca. 1.0 mmol·L^{-1} for the cobaloxime and 0.1 mol·L^{-1} for the supporting electrolyte, $(n\text{-}Bu_4N)BF_4$. Electrodes were polished on a MD-Nap polishing pad with 1 μm monocrystalline diamond DP suspension and DP lubricant blue (Struers). Additions of Et_3NHCl were made by syringe using a 50 mmol·L^{-1} solution in DMF. Bulk electrolysis and coulometry were carried out on a EG&G PAR 273A instrument in 1,2-dichloroethane, using a 2 cm^2 graphite cathode. The platinum-grid + carbon-foam counter electrode was placed in a separated compartment connected with a glass-frit and filled with a 0.3 mol·L^{-1} solution of $(n\text{-}Bu_4N)BF_4$ in degassed 1,2-dichloroethane. A degassed 1,2-dichloroethane solution (10 mL) containing 0.1 mol·L^{-1} $(n\text{-}Bu_4N)BF_4$ and 0.2 mol·L^{-1} $(Et_3NH)BF_4$ was first electrolyzed at −0.90 V/(Ag/AgCl) until the current has dropped below 1 mA. The catalyst (1.0 mmol dissolved in 500 μL of degassed dichloroethane) was added, and electrolysis was then performed at −0.90 V/(Ag/AgCl). Electrolysis cell constant was determined to be 2×10^{-4} s^{-1} by performing bulk electrolysis of ferrocene.[27] The faradaic yield was periodically estimated from the volumetric measure of the amount of evolved gas during the time needed for a 10 C of charge to pass through the cell. Hydrogen was tested for purity using a Delsi Nermag DN200 GC chromatograph equipped with a thermal conductivity detector (TCD) detector.

Cyclic voltammograms were simulated and best-fitted using Digisim[28] or DigiElch[29] software. A first simulation was performed for each catalyst in the absence of added acid. Parameters were refined until voltammograms recorded at 20, 100, and 500 mV·s^{-1} could be simulated using the same set of values. The resulting parameters were kept unchanged for simulation of voltammograms recorded in the presence of acid. The model was then modified to include the catalytic steps, and the new parameters were refined until one set of value could provide correct simulation of the voltammograms recorded in the presence of various amounts (1.5, 3, and 10 equiv) of added acid at 20, 100, and 500 mV·s^{-1}.

$[Co(dmgH)_2(4\text{-}(Me_2N)C_5H_4N)Cl]$. $CoCl_2 \cdot 6H_2O$ (500 mg, 2.15 mmol), dimethylglyoxime (551 mg, 4.70 mmol), and NaOH (86.0 mg, 2.15 mmol) were dissolved in 95% ethanol (20 mL) and heated to 70 °C. 4-(Dimethylamino)pyridine (263 mg, 2.15 mmol) was then added and the resulting solution cooled to room temperature. A stream of air was then passed through the solution for 30 min, which caused precipitation of a brown solid. The suspension was stirred for 1 h and filtered. The precipitate was successively washed with water (5 mL), ethanol (2 × 5 mL), and diethyl ether (3 × 5 mL). The product was then extracted with acetone. Removal of the solvent from the extracts yielded pure $[Co(dmgH)_2(4\text{-}(Me_2N)C_5H_4N)Cl]$ (465 mg, 1.04 mmol, 48%). Anal. Calcd for $C_{15}H_{24}N_6ClCoO_4$: C, 40.32; H, 5.41; N, 18.81; Cl, 7.94; Co, 13.19. Found: C, 41.77; H, 5.71; N, 17.74; Cl, 7.51; Co, 12.41. ^1H NMR (300 MHz, $CDCl_3$): δ 18 (broad, O*H*), 7.62 (d, $J = 6.6$ Hz, 2H, py), 6.28 (d, $J = 6.6$ Hz, 2H, py), 2.95 (s, 6H N*Me*$_2$), 2.38 (s, 12H, dmg^{2-}).

4-(*N*-*tert*-Butylcarboxamido)pyridine. *tert*-Butylamine (293 μL, 2.80 mmol) was added to a solution of isonicotinoyl chloride hydrochloride (500 mg, 2.80 mmol) and triethylamine (1.57 mL, 11.2 mmol) in THF (10 mL). The mixture was stirred overnight at room temperature and filtered. The solvent was removed, and the product was chromatographied on silica using $MeOH/CH_2Cl_2$ (1.2/98.8 (v/v)) as eluant. The product was recovered as a pure white powder (210 mg, 1.18 mmol, 42%). Spectroscopic data are similar to those previously described.[30]

$[Co(dmgH)_2(4\text{-}(t\text{-}BuNH(C{=}O)C_5H_4N)Cl]$. $CoCl_2 \cdot 6H_2O$ (278 mg, 1.17 mmol), dimethylglyoxime (298 mg, 2.57 mmol), and NaOH (47.0 mg, 1.17 mmol) were dissolved in 95% ethanol (10 mL) and heated to 70 °C. 4-(*N*-*tert*-butylcarboxamido)pyridine (208 mg, 1.17 mmol) dissolved in 95% ethanol (3 mL) was then added and the resulting solution cooled to room temperature. A stream of air was then passed through the solution for 45 min, which caused the precipitation of a brown solid. The suspension was stirred for 1 h and filtrated. The precipitate was successively washed with water (5 mL), ethanol (2 × 5 mL), and diethyl ether (3 × 5 mL). The product was then extracted with acetone. Removal of the solvent from the extracts yielded pure $[Co(dmgH)_2(4\text{-}(t\text{-}BuNH\text{-}(C{=}O))C_5H_4N)Cl]$ (306 mg, 0.61 mmol, 52%). Anal. Calcd for $C_{18}H_{28}N_6ClCoO_5$: C, 42.99; H, 5.61; N, 16.71; Cl, 7.05; Co, 11.72. Found: C, 43.33; H, 5.80; N, 17.57; Cl, 6.91; Co, 11.22. ^1H NMR (300 MHz, $CDCl_3$): δ 18 (broad, O*H*), 8.35 (d, $J = 6.4$ Hz, 2H, py), 7.46 (d, $J = 6.4$ Hz, 2H, py), 5.91 (s, 1H, N*H*t-Bu), 2.36 (s, 12H, dmg^{2-}), 1.38 (s, 9H, C*Me*$_3$).

Results

Electrocatalytic Activity of $[Co(dmgH)_2(py)Cl]$. The cyclic voltammogram of $[Co^{III}(dmgH)_2(py)Cl]$ recorded in DMF exhibits one irreversible reduction of Co(III) to Co(II) ($E_{pc} = -0.61$V/(Ag/AgCl)) followed by a reversible Co(II)/Co(I) process at −0.98 V/(Ag/AgCl). Addition of increasing amounts, i.e., 1.5, 3.0, and 10 equiv, of a weak acid, Et_3NH^+ ($pK_a = 10.75$), triggers the appearance of a new irreversible cathodic wave near the Co(II)/Co(I) response

(21) Gerli, A.; Marzilli, L. G. *Inorg. Chem.* **1992**, *31*, 1152.
(22) Bakac, A.; Espenson, J. H. *J. Am. Chem. Soc.* **1984**, *106*, 5197.
(23) Toscane, P. J.; Swider, T. F.; Marzilli, L. G.; Bresciani-Pahor, N.; Randaccio, L. *Inorg. Chem.* **1983**, *22*, 3416.
(24) Christensen, J. B. *Molecules* **2001**, *6*, 47.
(25) Mohamed, K. S.; Padma, D. K. *Indian J. Chem.* **1988**, *27A*, 759.
(26) Koepp, H. M.; Wedt, H.; Strehlow, H. *Z. Elektrochem.* **1960**, *64*, 483.
(27) Pletcher, D. *A first course in electrode processes*; The Electrochemical Consultancy: Hants, U.K., 1991.
(28) (a) Digisim 3.05 for Windows 95 distributed by the Bioanalytical Corp. (b) Rudolph, M.; Reddy, D. P.; Feldberg, S. W. *Anal. Chem.* **1994**, *66*, 589A.
(29) (a) Rudolph, M. *J. Electroanal. Chem.* **2003**, *543*, 23. (c) Rudolph, M. *J. Electroanal. Chem.* **2003**, *558*, 171. (c) Rudolph, M. *J. Electroanal. Chem.* **2004**, *571*, 289.
(30) Bonnet, V.; Mongin, F.; Trécourt,; Quéguiner, G. *J. Chem. Soc., Perkin Trans. 1* **2000**, 4245.

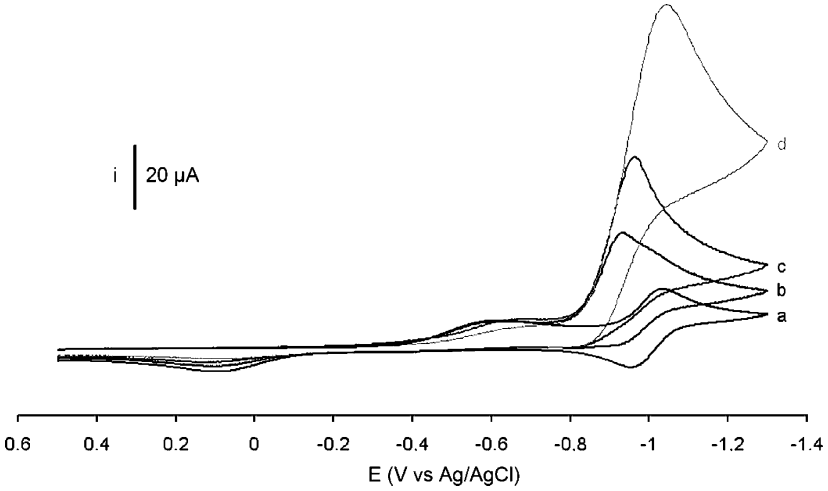

Figure 3. Cyclic voltammograms of $[Co(dmgH)_2(py)Cl]$ (1.0 mmol·L^{-1}) in the presence of various amounts of Et_3NHCl recorded in a DMF solution of *n*-Bu_4NBF_4 (0.1 mol·L^{-1}) on a glassy carbon electrode at 100 mV·s^{-1}: (a) 0 equiv; (b) 1.5 equiv; (c) 3.0 equiv; (d) 10 equiv (potentials versus Ag/AgCl).

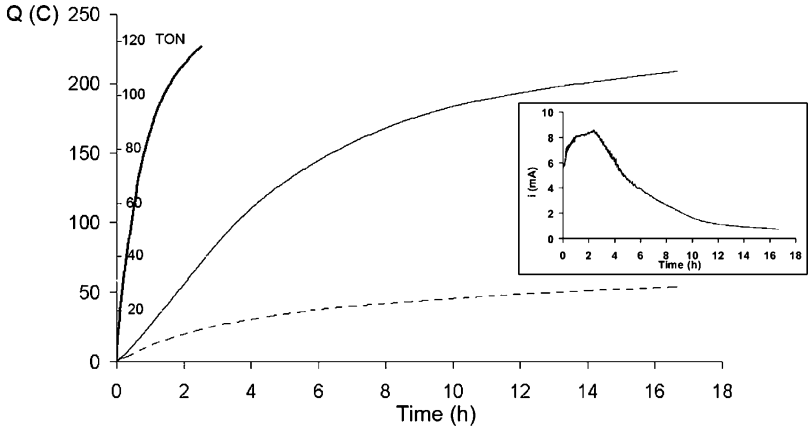

Figure 4. Coulometry for bulk electrolysis at −0.90 V/(Ag/AgCl) of a 1,2-dichloroethane solution of Et_3NHBF_4 (0.2 mol·L^{-1}) and *n*-Bu_4NBF_4 (0.1 mol·L^{-1}) at a graphite electrode in the presence of 1.0 mmol·L^{-1} Key: $[Co(dmgH)_2(py)Cl]$ (bold); $[Co(dmgBF_2)(OH_2)_2]$ (plain); without catalyst (dashed). Evolution of the current as a function of time during the same experiment in the case of $[Co(dmgBF_2)(OH_2)_2]$ is shown in the inset.

(Figure 3). The behavior of this new wave is typical of a "total" catalysis, as defined by Savéant et al.[31] and observed for [Fe(TPP)Cl] (TPP^{2-} = *meso*-tetraphenylporphyrinato) under the same conditions.[32] At low acid/catalyst concentration ratios, the catalytic wave lies at more positive potentials than that of the Co(II)/Co(I) couple. The latter is still observed as a shoulder when the voltammogram is recorded at 100 mV·s^{-1} (Figure 3) and is better defined at 20 mV·s^{-1} (Figure 5). Increasing the acid/catalyst concentration ratio raises the height of the new wave and shifts it to more negative potentials while the Co(II)/Co(I) reversible wave disappears. This catalytic wave can then be assigned to proton electroreduction. Bulk electrolysis on a graphite electrode at −0.90 V/(Ag/AgCl) of a 0.2 mol·L^{-1} solution of $Et_3NH(BF_4)$ in 1,2-dichloroethane[33] in the presence of 1.0 mmol·L^{-1} $[Co(dmgH)_2(py)Cl]$ produces H_2 gas, identified by gas chromatography, with a 85−100% faradaic yield. Electrolysis was complete after 2.5 h, corresponding to 100 ± 3 turnovers (193 C after subtraction of the blank electrolysis, Figure 4). No degradation of the catalyst is observed as shown by UV−visible spectroscopy.[34,35] The cathodic current decreases exponentially during electrolysis with a time constant identical with that of the electrolysis cell. Proton reduction electrocatalysis is therefore mass transport-controlled, and the measured turnover frequency (TOF) depends on the geometry of the electrochemical cell which can be improved a 100-fold by electrochemical engineering.[36] When the electrolysis is performed under the same conditions but in the absence of catalyst, the volume of evolved H_2 does not exceed 1 mL.

Tuning Redox Features. The effect of varying the electronic properties of the ligand on the catalytic activity was investigated. The electrochemical features of various

(31) (a) Andrieux, C. P.; Blocman, C.; Dumas-Bouchiat, J.-M.; M'Halla, F.; Savéant, J.-M. *J. Electroanal. Chem.* **1980**, *113*, 19. (b) Savéant, J.-M.; Su, K. B. *J. Electroanal. Chem.* **1984**, *171*, 341.

(32) Bhugun, I.; Lexa, D.; Savéant, J.-M. *J. Am. Chem. Soc.* **1996**, *118*, 3982.

(33) If electrolysis is carried out in DMF, the solution turns green and the current drops after one turnover.

(34) Reaction of $[Co(dmgH)_2py]$ with H_2 in MeOH yields 2-aminobutan-3-one oxime as a result of hydrogenation of dimethylglyoxime: Simándi, L. I.; Szeverényi, Z.; Budó-Záhonyi, E. *Inorg. Nucl. Chem. Lett.* **1975**, *11*, 773.

(35) At this point, proton electroreduction can be started again by adding of HBF_4·Et_2O (270 μL, 2.00 mmol) to the solution containing Et_3N after electrolysis of Et_3NHBF_4. This was repeated twice, yielding ∼300 TON without observation of catalyst degradation.

(36) Bard, A. J. *Anal. Chem.* **1963**, *35*, 1125.

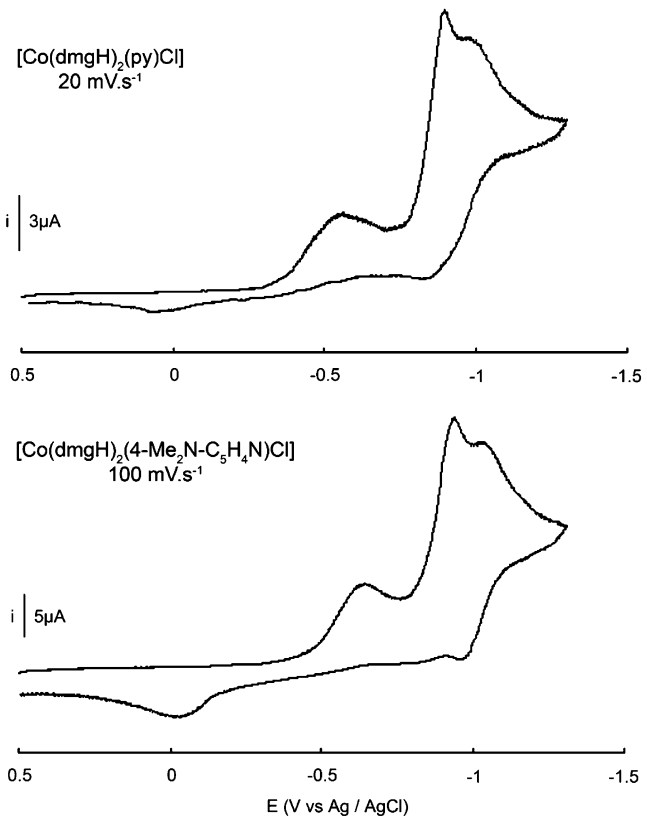

Figure 5. Cyclic voltammograms of 1.0 mmol·L^{-1} [Co(dmgH)$_2$(L)Cl] (top, L = py, 20 mV·s^{-1}; bottom, L = 4-Me$_2$NC$_5$H$_4$N, 100 mV·s^{-1}) + 0.1 mol·L^{-1} *n*-Bu$_4$NBF$_4$ in DMF at a glassy carbon electrode in the presence of Et$_3$NHCl (mmol·L^{-1}, 1.5 equiv).

cobaloxime derivatives containing different glyoxime ligands and axial bases are reported in Table 1.

Substitution of hydrogen or phenyl for methyl at the glyoxime ligands significantly increases the electrochemical potentials of the Co(II)/Co(I) couple as expected for less electron-donating ligands but also results in the loss of the proton reduction electroactivity on the cyclic voltametry time scale. The same effects are observed when substituting $\{BF_2\}^+$ for proton bridges between the equatorial ligands: the potential of the Co(II)/Co(I) couple in the cobalt(II) species [Co(dmgBF$_2$)$_2$(OH$_2$)$_2$] (−0.55 V/(Ag/AgCl) in DMF) is the highest in the series and thus the closest to that of the H^+/H_2 couple. Yet, the cyclic voltammogram of [Co(dmgBF$_2$)$_2$(OH$_2$)$_2$] is not modified upon addition of Et$_3$NHCl. This cannot exclude the possibility for [Co(dmgBF$_2$)$_2$(OH$_2$)$_2$] to be active toward Et_3NH^+ but may reflect that turnover frequency is low on the cyclic voltametry time scale.[37] Bulk electrolysis on a graphite electrode at −0.90 V/(Ag/AgCl) of a 0.2 mol·L^{-1} solution of Et$_3$NH(BF$_4$) in 1,2-dichloroethane in the presence of 1.0 mmol·L^{-1} [Co(dmgBF$_2$)$_2$(OH$_2$)$_2$] indeed produces H_2 gas, identified by gas chromatography, with a 75−100% faradaic yield. Electrolysis is almost complete after 17 h, corresponding to 80 ± 3 turnovers (155 C after subtraction of the blank electrolysis, Figure 4). No degradation of the catalyst is observed by UV−visible spectroscopy during the reaction.[38] As expected from the cyclic voltametry experiments, the cathodic current is smaller than that obtained in a similar experiment using [Co(dmgH)$_2$(py)Cl] as catalyst. The current initially increases, reaches a maximum, and then decreases exponentially with a time constant lower than that of the electrolytic cell (see inset in Figure 4), in agreement with *her* being controlled by turnover frequency and not by mass transport. The induction time probably corresponds to the formation of the active species in the bulk. The high current value measured during electrolysis is possibly due to higher amounts of the active species accumulating in the bulk as evidenced by the brown color of the solution after the induction time. This is in contrast with electrolysis experiments using [Co(dmgH)$_2$pyCl] for which the active species react immediately nearby the electrode with only a small part of the introduced complex actually achieving catalysis at the same time. According to the proposed mechanism for the reduction of HCl by divalent metal salts catalyzed by [Co(dmgBF$_2$)$_2$(OH$_2$)$_2$],[15] hydrogen evolution should occur when electrolysis is performed at −0.55 V/(Ag/AgCl) in DMF or 1,2-dichloroethane. In fact it does not until the electrolysis potential is lowered to −0.90 V/(Ag/AgCl). This may imply that the reaction with a weak acid such as Et$_3$NHCl proceeds via another mechanism where the Co(III)−hydride species formed at −0.55 V/(Ag/AgCl) should be activated by subsequent reduction at more negative potential. This system is currently under study.

Substitution at the axial positions would only be relevant if the introduced ligand is retained in the reduced Co(II) and Co(I) states. Whatever the scan rate used in the 20−2000 mV·s^{-1} range, the Co(III)/Co(II) system indeed appears always chemically irreversible, except for [Co(dmgH)$_2$(py)$_2$](PF$_6$) studied in pyridine as solvent: the reduction wave of the Co(III) species is broad and flattened, and its position depends on the polishing state of the electrode. The corresponding anodic wave on the reverse scan is shifted by 700 mV, consistent with an ECE mechanism (see eqs 1−3 in Scheme 1) involving an irreversible loss of an axial ligand to yield a pentacoordinated Co(II) species.[39] The cyclic voltammograms of [Co(dmgH)$_2$(py)X] (X = Cl$^-$ or I$^-$) and [Co(dmgH)$_2$(py)$_2$]$^+$ display Co(III)/Co(II) cathodic peaks at different potentials while the Co(II)/Co(I) reversible features (−0.98 V/(Ag/AgCl) and the Co(II)/Co(III) anodic peak (0.15 V/(Ag/AgCl) are found at the same potential indicating that in the reduced state axial halide ligands are more labile than pyridine. It should be noted that recombination of halide with the pentacoordinated cobaloxime is not immediate after

(37) The observation of an electrocatalytic property using cyclic voltametry is unfortunately restricted to fairly active species, i.e., with a second-order rate constant of more than approximately 100 mol·L^{-1}·s^{-1} as estimated by DuBois and co-workers: Curtis, C. J.; Miedaner, A.; Ciancanelli, R.; Ellis, W. W.; Noll, B. C.; DuBois, M. R.; DuBois, D. L. *Inorg. Chem.* **2003**, *42*, 216.

(38) If the electrolysis experiment is stopped before complete consumption of the acid, the color turns back to yellow and the final UV−visible spectrum is identical with the initial one. However, if the electrolysis experiment is continued after total depletion of the acid, the current drops and a green color develops. This color can be due to an alternative decomposition pathway of the reactive species, which is not observed as long as there is enough acid in the solution.

(39) Ngameni et al. previously reported reversible behavior for the Co(III)/Co(II) couple of [Co(dmgH)$_2$PyI] in CH$_3$CN: Ngameni, E.; Ngoune, J.; Nassi, A.; Megnamisi Belombe, M.; Roux, R. *Electrochim. Acta* **1996**, *41*, 2571. However, in our hand, this compound show irreversible chemical behaviour regarding the Co(III)/Co(II) couple.

Table 1. Electrochemical Potentials versus Ag/AgCl (V) Measured in DMF on a Glassy Carbon Electrode for Cobaloximes (Scan Rate: 100 mV·s^{-1})

	$E_{pc}(Co^{III}/Co^{II})$	$E_{pa}(Co^{III}/Co^{II})$ (reverse scan)	$(E_{pc}+E_{pa})/2(Co^{II}/Co^{I})$
$[Co^{III}(dmgH)_2(py)Cl]$	−0.59	0.15	−0.98
$[Co^{III}(dmgH)_2(4\text{-}Me_2NC_5H_4N)Cl]$	−0.66	0.06	−1.01
$[Co^{III}(dmgH)_2(4\text{-}t\text{-}BuNHCOC_5H_4N)Cl]$	−0.65	0.15	−0.97
$[Co^{III}(dmgH)_2(py)I]$	−0.44	0.15	−0.98
$[Co^{III}(dmgH)_2(py)_2](PF_6)$	−0.24	0.15	−0.98
$[Co^{III}(dmgH)_2(PBu_3)Cl]$	−0.62	0.24	−0.81
$[Co^{II}(dmgH)_2(OH_2)_2]$	0[a]	0.30	−0.98
$[Co^{II}(dmgBF_2)_2(OH_2)_2]$	*b*	0.40	−0.55
$[Co^{III}(gH)_2(py)Cl]$	−0.40	*b*	−0.65
$[Co^{III}(dpgH)_2(py)Cl]$	−0.47[c]	0.17	−0.70

[a] Second scan. [b] Not observed. [c] Unresolved in DMF but well defined in CH_3CN.

Scheme 1. Mechanism Used for Simulation of the Cyclic Voltammograms

$$[Co^{III}(dmgH)_2LX] + e^- \rightleftharpoons [Co^{II}(dmgH)_2LX]^- \quad (1)$$

$$[Co^{II}(dmgH)_2LX]^- \rightleftharpoons [Co^{II}(dmgH)_2L] + X^- \quad (2)$$

$$[Co^{III}(dmgH)_2L]^+ + e^- \rightleftharpoons [Co^{II}(dmgH)_2L] \quad (3)$$

$$[Co^{II}(dmgH)_2L] + e^- \rightleftharpoons [Co^{I}(dmgH)_2L]^- \quad (4)$$

$$[Co^{I}(dmgH)_2L]^- + H^+ \rightleftharpoons [Co^{III}(dmgH)_2LH] \quad (5)$$

$$[Co^{III}(dmgH)_2LH] + H^+ \rightleftharpoons [Co^{III}(dmgH)_2L]^+ + H_2 \quad (6)$$

$$2\,[Co^{II}(dmgH)_2L] \rightleftharpoons [Co^{I}(dmgH)_2L]^- + [Co^{III}(dmgH)_2L]^+ \quad (7)$$

reoxidation to the Co(III) state (reverse scan) since a new reduction wave at −0.15 V/(Ag/AgCl), presumably that of the pentacoordinated cationic $[Co(dmgH)_2(py)]^+$ species, can be observed if a second scan is immediately performed (see Supporting Information). This $[Co(dmgH)_2(py)]^+/[Co(dmgH)_2(py)]$ couple appears quasi-reversible with a peak-to-peak separation of 300 mV (Scheme 1, eq 3).

Substitution of tributylphosphine for pyridine in $[Co(dmgH)_2(py)Cl]$ increases the potential of the Co(II)/Co(I) couple to −0.81 V/(Ag/AgCl), but this also results in the loss of the electrocatalytic activity on the cyclic voltametry time scale.

Substitution of 4-(dimethylamino)pyridine or 4-(*N*-*tert*-butylamido)pyridine for pyridine in $[Co(dmgH)_2(py)Cl]$ does not result in a significant modification of the potential for the Co(II)/Co(I) couple as previously reported for alkyl cobaloximes,[40,45] but careful examination of the cyclic voltammograms recorded at low acid/catalyst ratios reveals that the more donating the axial ligand, the more active the catalyst. For 1−1.5 equiv of acid added, and at a scan rate of 100 mV·s^{-1}, the catalytic wave is well separated from the Co(II)/Co(I) wave in the case of $[Co(dmgH)_2(4\text{-}Me_2NC_5H_4N)Cl]$ (Figure 5) while these waves are merged for $[Co(dmgH)_2(py)Cl]$ (Figure 3) and could only be resolved at lower scan rate such as 20 mV·s^{-1} (Figure 5). As the potential shift observed for an EC mechanism is correlated with the reaction rate of the chemical reaction following electron transfer,[31,41] this indicates an increased catalytic activity (TOF) using 4-(dimethylamino)pyridine as the axial ligand.

(40) Rillema, D. P.; Endicott, J. F.; Papaconstantinou, E. *Inorg. Chem.* **1971**, *10*, 1739.

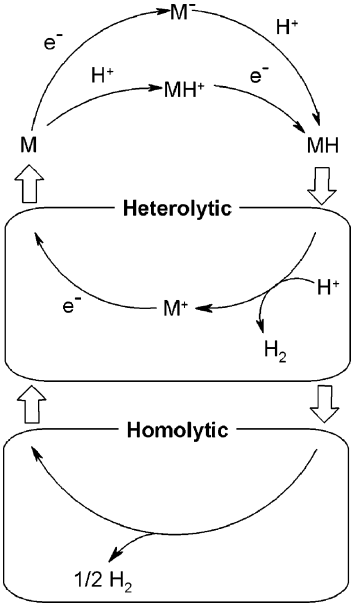

Figure 6. Heterolytic and homolytic pathways for proton reduction catalyzed by a coordination compound.

Mechanism Determination. Proton reduction yields dihydrogen following two general pathways depending on whether the H−H bond is formed via a homolytic or a heterolytic step. The general mechanistic schemes[3] are given in Figure 6.

Both catalytic cycles include protonation of the metal center to give a metal−hydride complex. In the homolytic mechanism, H_2 evolution results from a reductive elimination reaction from two metal−hydride moieties. In the heterolytic pathway, the metal hydride decomposes by proton attack to evolve hydrogen, probably via an intermediate dihydrogen−metal complex. The catalytic cycle is completed by one or two monoelectronic reduction steps which can occur either at the unprotonnated metal center or after formation of the hydride species.

Simulation of the voltammograms obtained for cobaloximes in the presence of triethylammonium chloride

(41) For an EC mechanism with reversible heterogeneous charge-transfer E (n = number of transferred electrons) and rapid chemical reaction (rate constant k) on the time scale of cyclic voltametry (scan rate, υ), the potential shift is given by the equation $E_p = E_{1/2} - 0.780(RT/nF) + (RT/2nF)\ \ln(kRT/nF\upsilon)$, so that the wave shifts toward positive potentials by about $30/n$ mV (at 25 °C) for a 10-fold increase of k (Bard, A., J.; Faulkner, L. R. *Electrochemical Methods*; Wiley: New York, 1980; p 452).

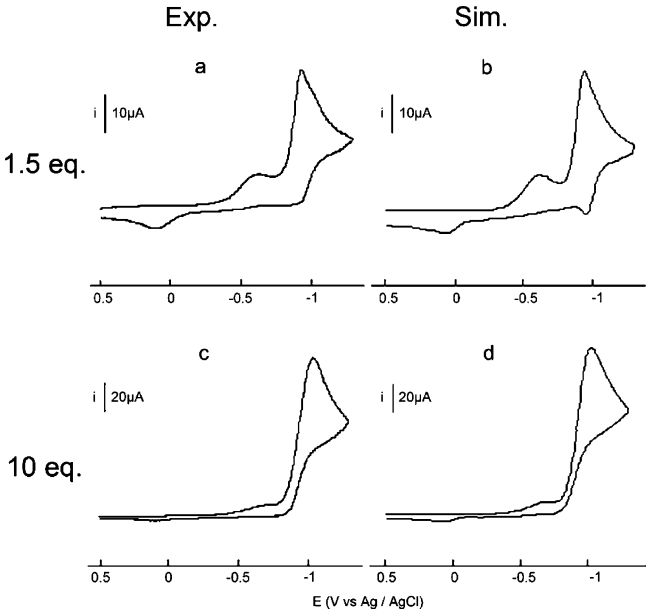

Figure 7. Cyclic voltammograms of $[Co(dmgH)_2(py)Cl]$ (top, 0.970 mmol·L^{-1}; bottom, 0.833 mmol·L^{-1}) recorded in DMF solution of *n*-Bu_4NBF_4 (0.1 mmol·L^{-1}) at a glassy carbon electrode in the presence of Et_3NHCl (top, 1.46 mmol·L^{-1}, 1.5 equiv; bottom, 8.33 mmol·L^{-1}, 10 equiv). Scan rate: 100 mV·s^{-1}. Left: experimental curves. Right: simulated curves.

allowed us to assign a heterolytic nature to the mechanism. With the homolytic hypothesis, the simulated electrocatalytic wave indeed displays a peculiar shape with a round toped peak (see Supporting Information), whereas the classical, experimentally observed, sharp pointed peak is observed for the heterolytic model. Furthermore, using a model including both mechanisms, a very low kinetic constant is obtained for the homolytic step compared to the reaction rates of the heterolytic steps, indicating that the contribution of the homolytic mechanism is minor if any.

The relative order of the two one-electron transfer and two protonation steps in the heterolytic mechanism can be immediately determined by a simple examination of the voltamogram. If the electrocatalytic wave develops at potentials more negative than the reduction potential of the catalyst, it implies that the hydride moiety formed by protonation after reduction of the catalyst should still be activated by further reduction. On the contrary, an electrocatalytic wave developing at potential just above a reduction wave of the catalyst attests for the two one-reduction steps occurring before the two protonation steps. This is the case for proton reduction catalyzed by cobaloximes. Such a mechanism was also ascertained using cyclic voltammetry by Savéant et al. for proton electroreduction catalyzed by iron[32] and rhodium[42] porphyrin complexes.

We thus simulated the voltammograms using the mechanism given in Scheme 1 and were able to reproduce the experimental data (Figure 7). As seen in Figure 7, the major discrepancies between simulated and experimental value concern the reverse scan, namely the anodic peak related to the Co(II)/Co(I) couple at low acid concentrations. This peak is better defined in the simulations than in the experimental data. We suppose that this is a consequence of the modification of the surface state of the electrode upon electrocatalysis, which is not taken into account in the model. Indeed, this anodic peak is better resolved when the cyclic voltammogram is recorded on a hanging mercury electrode (data not shown). We have chosen height, position, and shape of the catalytic wave as relevant criteria for the evaluation of the simulation. Significant extracted data are given in Table 2.

Charge-transfer parameters ($E°$, α, k_s) and diffusion coefficients corresponding to eqs 1, 3, and 4 and thermodynamic (K_{eq2}) and kinetic (k_{f2}) parameters for eq 2 were determined using voltammograms of cobaloximes without any added acid and kept unchanged for further simulation in the presence of acid. Heterogeneous charge-transfer processes appear relatively slow with rate constants k_s ranging from 10^{-3} to 10^{-2} cm·s^{-1}. Equation 2 is a total reaction with a first-order rate constant ranging from 10^5 to 10^9 s^{-1}. Disproportionation reaction 7 was set as diffusion-controlled. Its equilibrium constant was calculated from the standard potentials of the corresponding redox couples. Introduction of this reaction in our model led to a better, even not optimal (see above), graphical reproduction of the reverse scan of the electrocatalytic wave.

The value of the product $K_{eq5}K_{eq6}$ was estimated as 2×10^9 using the method of Spiro et al.[16] and fixed during simulations. Simulation showed that both reactions 5 and 6 are fully shifted except in the case of the amido derivative $[Co(dmgH)_2(4\text{-}t\text{-}BuNHC(=O)C_5H_4N)Cl]$ for which a K_{eq5} value of 400 was found, in accordance with the electron-withdrawing property of the amido group.

Reaction 6 was found to be kinetically determinant. The value of its rate constant k_{f6} determines the height of the electrocatalytic wave while the reaction rate constant of eq 5 coupled with the heterogeneous charge-transfer rate constant k_{s4} is responsible for the position of the electrocatalytic wave. Only a lower limit for k_{f5} at 10^8 mol^{-1}·L·s^{-1} can be determined since higher values do not modify the simulated voltammogram. Ammonium ions being more acidic than water, this value is in accordance with the lower limit at 10^4 mol^{-1}·L·s^{-1} determined by Spiro et al. for the reaction rate of Co(I) porphyrin centers with water.[16a]

The same simulation and best fitting was undertaken for $[Co^{II}(dmgH)_2(OH_2)_2]$ with a new model in which eqs 1−3 were deleted and assuming rapid substitution of one water molecule for the hydride ligand. Significantly lower values for k_{f5} (10^4 mol^{-1}·L·s^{-1}) and k_{f6} (300 mol^{-1}·L·s^{-1}) were obtained.

Selected parameters gained from simulations are reported in Table 2.

Discussion

In this study, we have reinvestigated the potential of cobaloximes for the hydrogen evolution reaction (*her*). Our results definitively show that $[Co(dmgH)_2LX]$ (L = pyridine derivatives, X = halide or labile ligands) are efficient and robust electrocatalysts:

(42) Grass, V.; Lexa, D.; Savéant, J.-M. *J. Am. Chem. Soc.* **1997**, *119*, 7526.

Table 2. Relevant Data Extracted from Simulation of the Voltammograms

catalyst	$E°_{Co(II)/Co(I)}$ (V/(Ag/AgCl))	k_{f5min} ($mol^{-1}·L·s^{-1}$)	K_{eq5}	k_{f6} ($mol^{-1}·L·s^{-1}$)	k_{f2} (s^{-1})
$[Co^{III}(dmgH)_2pyCl]$	−0.98	10^8	5×10^4	1.35×10^4	10^8
$[Co^{III}(dmgH)_2(4\text{-}Me_2NC_5H_4N)Cl]$	−1.01	10^8	5×10^4	2.5×10^3	10^9
$[Co^{III}(dmgH)_2(4\text{-}t\text{-}BuNHC(=O)C_5H_4N)Cl]$	−0.97	10^8	4×10^2	5×10^5	10^5
$[Co^{II}(dmgH)_2(OH_2)_2]$	−0.98	10^4	10^3	3×10^2	

Table 3. Comparison of Reported *Her*-Catalyst Properties

catalyst	appl potential	electrode	exptl conditns	TON	ref
poly{pyrrole-$[Cp*Rh(bipy)Cl]^+$} film	−0.55 V/SCE	glassy carbon	pH 1−4 aq soln	353 (14 h)	13c
[CoPc]/poly(4-vinylpyridine-*co*-styrene)	−0.90 V/(Ag/AgCl)	basal-plane pyrolytic graphite	0.1 $mol·L^{-1}$ pH 1.0 phosphate buffer	$2 \times 10^5·h^{-1}$ [a]	44
$[Co(dmgH)_2pyCl]$	−0.90 V/(Ag/AgCl)	graphite	1,2-$C_2H_4Cl_2$−0.2 $mol·L^{-1}$ Et_3NHCl	100 (2.5 h)	this work
Co(TMAP),Co(TMPyP, CoTPyP	−0.95 V/SCE	Hg pool	aq 0.1 $mol·L^{-1}CF_3COOH$	0.65 (20 min)	16
$[Fe_2(\mu\text{-ADT})(CO)_6]$ [b]	−1.48 V/(Fc/Fc^+)	glassy carbon	CH_3CN−50 $mmol·L^{-1}$ $HClO_4$	25 (10 min)	9
$[Ni(L_{N4})]^+$ [c]	−1.1 V/SCE	glassy carbon	pH 2 aq soln	12.7 (12 h)	50
$[CpCo\{P(OMe)_3\}_2]$	−1.15 V/SCE	Hg pool	pH 5 aq soln	20 (18 h)	51
$[Ru_2(C_6H_3(CF_3)_2)_2DPB]$	−1.2 V/Ag	Hg pool	THF + CF_3COOH	1.6 (20 min)	52
$[HFe_2(\mu\text{-pdt})(CO)_4(CN)(PMe_3)]$ [d]	−1.2 V/(Ag/AgCl)	Hg pool	CH_3CN−50 $mmol·L^{-1}$ H_2SO_4	6 (15 min)	6c
$[Ni_2(biscyclam)]^{4+}$	−1.5 V/SCE	Hg pool	0.2 $mol·L^{-1}$ pH 7 phosphate buffer	100	14
[FeTPPCl]	−1.6 V/SCE	Hg pool	DMF−50 $mmol·L^{-1}$ Et_3NHCl	24 (1.25 h)	32

[a] Only TOF is reported for this complex. [b] ADT^{2-} = *p*-Br-$C_6H_4CH_2N(CH_2S)_2^{2-}$. [c] L_{N4}^- = 2,6-$(HN(CH_2)_3N{=}C(CH_3))_2C_5H_3N^-$. [d] pdt^{2-} = propane-1,3-dithiolate.

(i) They are active toward weak acids such as Et_3NH^+.

(ii) Their activation overpotentials are low. Proton electroreduction catalyzed by $[Co(dmgH)_2pyCl]$ occurs at potentials between −0.91 (1.5 equiv, $[Et_3NHCl]$ = 1.46 $mmol·L^{-1}$) and −0.98 V/(Ag/AgCl) (10 equiv, $[Et_3NHCl]$ = 8.30 $mmol·L^{-1}$) in DMF at a carbon electrode. Proton reduction of an Et_3NHCl solution occurs at a freshly polished platinum electrode in DMF at −0.88 V/(Ag/AgCl) ($[Et_3NHCl]$ = 1.46 $mmol·L^{-1}$) and −0.95 V/(Ag/AgCl) ($[Et_3NHCl]$ = 8.30 $mmol·L^{-1}$). This allows an estimation of a 30 mV overpotential for *her* catalyzed by $[Co(dmgH)_2(py)Cl]$.[43]

(iii) High turnover numbers could be obtained without any detectable decomposition of the catalyst as shown by UV−visible spectroscopy.

Moreover, the catalytic mechanism was elucidated using simulation of cyclic voltammograms. Hydrogen evolution proceeds via a heterolytic pathway with the key step consisting in the fairly rapid protonation of a cobalt(III)−hydride moiety (Table 2) as compared to the similar reaction of $[HFe^{II}(TPP)]^-$ with Et_3NH^+ (k = 4 10^5 $mol^{-1}·L·s^{-1}$).[32]

Comparison of a given *her* catalyst with others always proves difficult because the assay conditions described in the literature are different. Nevertheless cobaloximes appear superior to other first-row transition metal *her* catalysts which function at more negative potentials and/or at lower pH (Table 3). The rhodium and therefore unsustainable complex $[Cp*Rh(bipy)Cl]^+$,[13] active at the Rh(I) oxidation state, still works at a less negative potential. It is interesting to note that the [Fe]-only hydrogenase model compound bearing a derivative of the biological azadithiolate bridging ligand $[Fe_2(\mu\text{-ADT})(CO)_6]$ is an active *her* electrocatalyst working at moderate potential (−1.48 V/(Fc/Fc^+) corresponding to −1.03 V/(Ag/AgCl)).[9] However, $[Fe_2(\mu\text{-ADT})(CO)_6]$-catalyzed *her* is studied in 50 $mmol·L^{-1}$ perchloric acid solutions and reduction of protons under these conditions at a freshly polished platinum electrode occurs in our hands at −0.67 V/(Fc/Fc^+), which unfortunately still reveals an important (810 mV) activation overpotential. Cobalt porphyrins may be considered as good catalysts for H_2 evolution especially in neutral aqueous solution because of their high working potential and nucleophilicity, but their utilization is precluded by their tendency to adsorb on all electrode materials with subsequent loss of electrocatalytic properties.[16] Cobalt(II) phthalocyanine incorporated in a poly(4-vinylpyridine-*co*-styrene) film catalyzes proton electroreduction at −0.90 V/(Ag/AgCl) but in quite acidic conditions (pH 1).[44] The very high reported turnover frequency as compared to other electrocatalysts studied in the bulk is probably due to the fact that cobalt(II) phthalocyanine is grafted at the electrode.

Starting from the promising and simple catalyst $[Co(dmgH)_2pyCl]$, we then tried to improve it regarding both working potential and stability.

Increasing the electrochemical potential substantially remains essential in the perspective of an aqueous application, through immobilization of catalysts at an electrode surface, where the −0.413 V/SHE value for the apparent potential of the H^+/H_2 couple at pH 7 would apply. Some modifications of the coordination sphere of the cobalt ion reported here resulted in increased potential of the Co(II)/Co(I) wave (Table 1) but also in the parallel loss of the electrocatalytic wave. In fact, species with more positive reduction potentials are also less nucleophilic and thus exhibit significant catalytic activity only under strongly acidic conditions. As an example, 330 mV is gained in reduction potential when substituting

(43) The apparent pH in nonaqueous media is not well defined, and proton reduction electrocatalysis is most probably a general rather than a specific acid catalysis; i.e., the rate of the overall reaction depends not only on the apparent pH but also on the pK_a of the acid used in the assay. Thus, we believe that the potential of electrocatalyzed proton reduction should not be compared to the apparent potential for the H^+/H_2 couple at the given pH but rather to the electrocatalytic potential obtained under the same conditions on a platinum electrode, where the H^+/H_2 couple is likely to display the most Nerstian behavior.

(44) Zhao, F.; Zhang, J.; Abe, T.; Wöhrle, D.; Kanedo, M. *J. Mol. Catal. A* **1999**, *145*, 245.

glyoximato for dimethylglyoximato in $[Co^{II}(dmgH)_2(py)]$, but $[Co(gH)_2(PBu_3)]^-$ has been reported to be approximatively 600 times less nucleophilic than $[Co(dmgH)_2(PBu_3)]^-$.[23]

The remarkable stability of $[Co(dmgBF_2)_2(OH_2)_2]$[45] compared to $[Co(dmgH)_2pyCl]$ is worth being considered in the perspective of higher turnover number applications: in contrast with other proton-linked cobaloximes which decompose in a matter of minutes under acidic conditions, the half-life of $[Co(dmgBF_2)_2(OH_2)_2]$ in 0.05 mol·L^{-1} H^+ is 5.5 h.[45] Replacing protons with $\{BF_2\}^+$ linking groups in cobaloximes thus dramatically increases their stability toward hydrolysis.[22] Despite the absence of electrocatalytic wave in cyclic voltametry experiments, bulk electrolysis experiments carried out under the same conditions as for $[Co(dmgH)_2pyCl]$ amazingly revealed promising activity for *her*. $[Co(dmgBF_2)_2(OH_2)_2]$ therefore appears to be a good starting point for the design of acid-resistant cobaloxime-based electrocatalyst, and its solubility in water opens new and tantalizing fields of investigation, currently under study.

Bulk electrolysis experiments, using $[Co(gH)_2pyCl]$ or $[Co(dmgH)_2(PBu_3)Cl]$ as catalysts, revealed activities lower than or comparable to that of $[Co(dmgBF_2)_2(OH_2)_2]$. This is in accordance with former studies reporting protonation of $[Co(dmgH)_2(PBu_3)]^-$ to yield $[Co(dmgH)_2(PBu_3)H]$,[46] which evolves dihydrogen by parallel heterolytic and homolytic mechanisms.[19] With comparable activity but greater instability with respect to $[Co(dmgBF_2)_2(OH_2)_2]$, these species are therefore less attractive as electrocatalysts for *her*.

Although it seems difficult to increase the potential of cobaloximes without lowering their catalytic activity, the nucleophilicity of the cobalt(I) center can be significantly enhanced through substitution at the pyridine ligand and this without dramatically decreasing the potential of the Co(II)/Co(I) couple (Table 1). Introduction of the electron-donating dimethylamino substituent in *para* position of the axial pyridine increases the rate constant of the reaction 6 40-fold. The electron-withdrawing *N-tert*-butylamido substituent decreases this rate constant 5-fold. This effect can be linearly correlated to the Hammett coefficients which reflect the electronic properties of the substituents (Figure 8).[47] The resulting linear free enthalpy of activation correlation (Hammett equation) has a positive slope, in accordance with a nucleophilic attack of the cobalt(III)−hydride moiety toward protons (Scheme 1, eq 6). However, no effect of the axial ligand is observed in bulk electrolysis or rotating-disk experiments using $[Co(dmgH)_2(L)Cl]$ (L = py, 4-*t*-$BuNHCOC_5H_4N$ and 4-$Me_2NC_5H_4N$) as catalysts probably because the current response is mass transport-controlled. Nevertheless, technological applications for H_2 production with optimized mass transport should benefit from the axial ligand influence on the turnover frequency.

In another catalytic application, Lehn et al. used $[Co(dmgH)_2(OH_2)_2]$ under irradiation in combination with

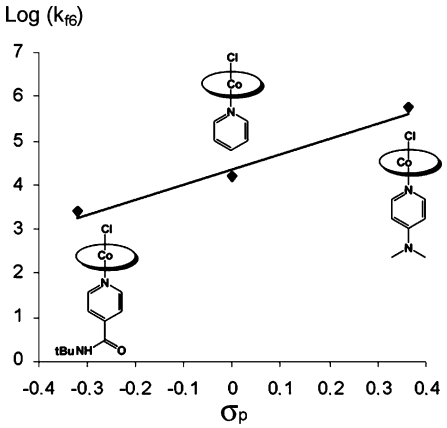

Figure 8. Logarithmic plot and linear correlation of the rate constant of eq 6 versus Hammet coefficients of the *para* substituent of the axial pyridine ligand L in $[Co(dmgH)_2(L)Cl]$.

$[Ru(bipy)_3]^{2+}$ and triethanolamine as the reducing source.[15b] Degradation (hydrogenation) of the catalyst was observed, and a 6-fold excess of dmgH was systematically added to maintain an active complex. Typical experiments were conducted in DMF and the pH (optimal value 8.9) was adjusted through addition of acetic acid or dissolution of carbon dioxide. The system was described as highly active but insufficiently stable in a long term use. Surprisingly, $[Co(dmgH)_2(OH_2)_2]$ was the less active cobaloximes of our study. Although cobaloximes bearing a pyridine as the axial base are described to be more sensitive to hydrogenation of the ligand,[34] we did not observe such a degradation when carrying out electrolysis in 1,2-dichloroethane or propylene carbonate. We hence believe that it should be worth reinvestigating such systems for hydrogen photoproduction, either using separated catalysts and photosensitizers[48] or designed bifonctional complexes.[49]

Conclusion

Cobaloxime complexes are valuable catalysts for proton electroreduction at moderate working potentials and in neutral conditions. Readily available from a one-step synthesis starting from classical chemicals of little value, they can be handled in air in the Co(III) state. Drawbacks could reside in their instability toward acid (pH < 5) even if highly acidic conditions are not a specification for *her* applications. Their activity and stability can be increased by modification of the axial or equatorial substituents, respectively. We are currently investigating the grafting of these species at graphite or glassy carbon electrode to develop heterogeneous aqueous applications.

Acknowledgment. The authors thank Eric Saint-Aman (LEOPR, University Joseph Fourier, Grenoble, France) and

(45) Lance, A. K.; Goldsby, K. A.; Busch, D. H. *Inorg. Chem.* **1990**, *29*, 4537.
(46) Schrauzer, G. N.; Holland, R. J. *J. Am. Chem. Soc.* **1971**, *93*, 1505.
(47) σ_p values were found in the following: *Correlation Analysis in Chemisry: recent advances*; Chapman, N. B., Shorter, J., Eds.; Plenum Press: New York, 1978; pp 439−540.
(48) Kirch, M.; Lehn, J.-M.; Sauvage, J.-P. *Helv. Chim. Acta* **1979**, *62*, 1345.
(49) (a) Komatsuzaki, N.; Himeda, Y.; Hirose, T.; Sugihara, H.; Kasuga, K. *Bull. Chem. Soc. Jpn.* **1999**, *72*, 725. (b) Balzani, V.; Juris, A.; Venturi, M. *Chem. Rev.* **1996**, *96*, 759.
(50) Efros, L. L.; Thorp, H. H.; Brudvig, G. W.; Crabtree, R. H. *Inorg. Chem.* **1992**, *31*, 1722.
(51) Kölle, U.; Ohst, S. *Inorg. Chem.* **1986**, *25*, 2689.
(52) Collman, J. P.; Ha, Y.; Wagenknecht, P. S.; Lopez, M.-A.; Guilard, R. *J. Am. Chem. Soc.* **1993**, *115*, 9080.

Martial Billon (DRFMC/SPrAM, CEA-Grenoble, France) for helpful discussions about voltammograms simulations, Jean-Marc Moulis and Jacques Meyer (DRDC/BMC, CEA-Grenoble, France) for the gift of a GC chromatograph, and Alexandra Ferrignio for performing the first experiments of this study during an undergraduate training in the laboratory.

Supporting Information Available: Experimental data and simulations, including parameters, using Digisim, and cyclic voltammograms of the supporting electrolyte (blank experiment), Et_3NHCl, and $[Co(dmgH)_2pyCl]$ (2 scans). This material is available free of charge via the Internet at http://pubs.acs.org.

IC050167Z